Centre for Building Studies

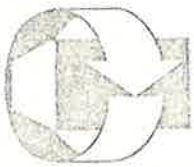

THE USE OF A BUILDING ENCLOSURE SIDING AS A PASSIVE COOLING DEVICE

Concordia University
Montreal, Quebec

by

Hiroshi Homma

and

Richard W. Guy

1455 de Maisonneuve Blvd. West
Montreal, Quebec, Canada H3G 1M8
(514) 879-8551

Report No. CBS-87

November, 1979

#2031

THE USE OF A BUILDING ENCLOSURE SIDING AS A PASSIVE COOLING DEVICE

by

Hiroshi Homma *

and

Richard W. Guy

CENTRE FOR BUILDING STUDIES
Concordia University
1455 de Maisonneuve Boulevard, West
Montréal, Québec

Presented at

D.E. ASHRAE CONFERENCE,
Orlando, Florida
December 3-5, 1979

Report NO. CBS-87

November, 1979

* Presently at TOYOHASI UNIVERSITY OF TECHNOLOGY, Toyohashi, Japan

ABSTRACT

The effect of ventilating the space between a main wall and an exterior metallic siding is examined with respect to reducing the building's cooling load. The buoyant force of the air in the space is considered as the motive force of air flow and the effect is treated as a problem of simultaneous heat and mass-transfer.

A simulation program of heat and air flows in a vertical air gap has been developed using laminar flow theory, and its validity is examined by the comparison of the simulation results with results obtained from a weather exposed full-scale model.

The computer simulation suggests that the ventilation of air spaces has the potential to reduce the radiative heat gain of both opaque walls and of triple glass windows.

1. INTRODUCTION

When louvers or shade devices are on the outside of a building envelope, most of the absorbed solar radiation is released to the outside from both sides of the device and the cooling load of the building is reduced; however, the use of such devices is limited for technical and architectural reasons.

In a similar fashion, when the back space of an exterior siding is ventilated the siding can also be cooled from its inner surface, and heat transmission into the main building enclosure could be reduced. As a siding absorbs solar radiation, its surface temperature rises, thus heating the air in the backing space. For example, the temperature of air in the backing space of a lightweight metal siding has been found to be 30°C higher than ambient outdoor air; in consequence, gravitational or buoyant forces, if allowed to develop, will have a significant effect in ventilating the backing space and thereby reduce the building's solar gain.

This ventilation effect was examined by developing a computer simulation of the air movement and heat flow in a vertical space. The results from this simulation were then compared with experimental results from a full-scale model.

The ventilation effect of an air space on the thermal performance of various wall and window structures are also examined by the simulation program and the results suggest their potential for passive reduction of a building's solar gain.

2. MATHEMATICAL MODEL

When solar radiation is absorbed in a siding located in front of an air gap and wall, the heat gain is transferred to air on both sides of the siding. When the air in the back space of the siding is warmer than outside air, buoyancy forces work on the air in the space to make it rise. As this movement develops, frictional force at the enclosing surface boundaries and inertia forces combine to oppose the buyoancy force; subsequently, the air movement in this space stabilizes at a velocity for which the three forces balance.

The heat balance in the space is maintained by heat exchange between the side walls and air, and the heat transportation by air flow; consequently, both heat and mass exchange will ultimately dictate the air space temperature. For a balanced condition of air movement and heat flow, heat and force balances must be treated simultaneously (Fig. 1). In a laminar flow range, the Newton's theory of frictional force can be applied, and here it is assumed to be applicable.

Typically, the overall siding width is much larger than the depth of the air space, and the temperature and flow field may be assumed twodimensional; the simulation program is accordingly based on the theory of two-dimensional heat and fluid flow [2,3].

The air space may now be divided into many thin vertical control layers, each of which are parallel to bounding surfaces. When the surface temperature on both sides of the air space is higher than the outdoor air, the temperature of the air which flows into the space increases gradually jnd rises.

Naturally, heat loss also occurs from the outer siding surface, either by forced convection (wind), natural convection, and/or re-radiation; however, these losses will not be considered in the development of the present analytical model.

2.1 Balance of Energy

The temperature distribution in the air space is calculated as follows: With respect to (Fig. 2), the very thin control layers in the air space are horizontally divided into small sections of height h. The heat q_1 conducted from the next space into the control space under consideration, is a function of the interface area $W.h$, the distance of centers of the two control spaces d, the conductivity K of the air, and the temperature difference Δt, as given by :

$$q_1 = W \cdot h \cdot K \cdot \frac{\Delta t}{d} \qquad (1)$$

where :

W is the width of the air space.

With the air flow parallel to the walls, the heat q_2 supplied by the air flow into the space under consideration is :

$$q_2 = Cp\ \rho\ V \cdot (t_i' - t_i)\ W \cdot d \qquad (2)$$

where :

t_i' and t_i are, respectively, the temperature of the air which flows into, and out of the i^{th} control space;

Cp is the specific heat of the air;

ρ is the density of the air; and

V is the air velocity.

The control layers are now assigned suffixes i's, and the vertically divided sections are designated by suffixes j's, the heat balance equation in the control space at the i^{th} layer and j^{th} section is :

$$\left(\frac{t_{i-1,j}-t_{i,j}}{\frac{d_{i-1}+d_i}{2}} + \frac{t_{i+1,j}-t_{i,j}}{\frac{d_i+d_{i+1}}{2}}\right) K.W.H. + \left(\frac{t_{i,j-1}-t_{i,j}}{\frac{h_{i-1}+h_i}{2}} + \frac{t_{i,j-1}-t_{i,j}}{\frac{h_i+h_{i+1}}{2}}\right) K.W.d_i$$

$$+ Cp\ \rho\ V_i\ (t_{i-1,j}-t_{i,j})\ W.d_i = 0 \qquad (3)$$

2.2 Heat Flow from Walls

The surface of each air space is treated, ideally as a single layer wall. The equivalent heat conductance is calculated from the series of thermal conductances of every layer for each wall, and the heat transfer by convection and radiation are treated separately on each of the four surfaces of the two walls.

The walls are also divided into 20 horizontal sections, in the same manner as the division of the air layers. The heat transfer between a section of a wall surface and the contacting air layer is, subsequently, assumed to take place separately for each of the sections.

The heat exchange between a wall surface and the air layer, which contacts the surface, is by conduction. The absorbed heat in the layer is partly conducted to the neighbouring layer, and partly transported by the air movement. Vertical heat transmission through a wall is neglected.

2.3 Balance of Forces

The buoyant pressure which works on the i^{th} control layer is the difference between the gravitational pressure of this control layer, and of the outside air column at the same height. This pressure is a function of the air density which may be expressed as a function of the temperature by:

$$\rho_j = \rho_r \frac{273 + t_r}{273 + t_j}$$

where :

ρ is density in Kg/m^3; and

t is temperature in °C of the air.

Suffixes j and r correspond respectively to the air in the layer and to the reference air. When an air layer of the height, H, is vertically divided into n sections, and the temperature and height of each section is expressed by t_j and h_j (j = 1 through n), respectively, the gravitational pressure P_l which is caused by this air layer is the summation of the gravitational pressures of every section; thus :

$$P_l = \sum_{j=1}^{n} h_j g \rho_r \frac{273 + t_r}{273 + t_j} = g\rho_r \sum_{j=1}^{n} h_j \frac{273 + t_r}{273 + t_j}$$

When the outside air temperature space is constant, t_o, then the gravitational pressure P_2, caused is :

$$P_2 = g\rho_r H \frac{273 + t_r}{273 + t_o}$$

The difference in the two pressures P_1 and P_2 is the buoyant pressure P_i, which is the motivational force to move the air in the i^{th} control layers; thus :

$$P_i = P_1 - P_2 = g\rho_r \left(\sum_{j=1}^{n} h_j \frac{273 + t_r}{273 + t_j} - H \frac{273 + t_r}{273 + t_o}\right) \qquad (4)$$

When an air mass is accelerated from the outside still condition to a velocity v in the air space, the mass attains a dynamic force. Some part of the buoyant pressure is converted into dynamic pressure to accelerate the air mass, and this dynamic pressure P_d is given by :

$$P_d = \frac{1}{2} \rho_o v^2 \qquad (5)$$

where :

ρ_o is the density of the outside air.

The frictional force, which is caused on an air layer by contact with the two neighbouring layers is calculated from Newton's law.

The velocities of $(i-1)^{th}$, i^{th} and $(i+1)^{th}$ layers are expressed by v_{i-1}, v_i and v_{i+1}, respectively; the frictional force F_f, which is caused on the i^{th} layer by the $(i-1)^{th}$ and $(i+1)^{th}$ layers is :

$$F_f = \left\{ \frac{v_{i-1} - v_1}{\frac{d_{i-1}+d_i}{2}} + \frac{v_i - v_{i+1}}{\frac{d_i+d_{i+1}}{2}} \right\} \rho \text{ H.W.} \qquad (6)$$

where :

ρ = is the dynamic viscosity of the air;

d_{i-1}, d_i and d_{i+1} are the thicknesses of $(i-1)^{th}$, i^{th} and $(i+1)^{th}$ layers.

The force F_b, which is caused on the i^{th} layer by the residual of the buoyant pressure subtracted of the velocity pressure, is the product of the horizontal sectional area of the air layer and the residual pressure as

$$F_b = W \times d_i \times (P_i - P_d)$$

$$= W \times d_i \times \left(g\rho_r \left(\sum_{j=1}^{n} h_j \frac{273 + t_r}{273 + t_j} - H \frac{273 + t_r}{273 + t_o} \right) - \frac{1}{2} \rho_o v^2 \right) \qquad (7)$$

When the motivational force F_b balances with the frictional force F_f, the flow of the i^{th} air layer stabilizes, as :

$$F_b = F_f \qquad (8)$$

The equation of force balance (8) is established for each layer in the air space.

When a siding is attached to the exterior of a wall, the vertical air passage between the siding and wall is restricted by the framework. The dynamic force of the air movement is calculated by using the maximum air velocity in the air space, and the volumetric flow rate is calculated from the velocity distribution in an air space. The maximum velocity is calculated by dividing the volumetric flow rate in the area of the most restricted part of the air passage, for example the opening at the bottom of the air space in Fig. 1. The dynamic force is assumed to distribute evenly over each air layer.

2.4 Solving Heat and Air Flow in an Air Space

To attain a balanced condition of heat and air flow in an air space, the equations of heat and force balance must be solved simultaneously. The heat balance equation (3) is set for each of the control spaces and wall sections, and the force balance equation (8) is set for each control layer.

As the number of unknowns are large, and the equation of force balance is a binomial equation of air velocity, the solution cannot be attained directly. The balanced condition is sought by successively correcting the velocities and temperatures of the control spaces by optimization techniques, starting from roughly estimated velocity and temperature distributions.

A computer program was developed to process these equations. In this program, an air space is divided into eleven vertical sections, and into twenty equal spaces. The thickness of the layers are changed to attain a

better simulation result. In the neighbourhood of a wall surface, the temperature and velocity gradients are larger than in the central part of an air space. The thickness of the control layers was set thinner in the periphery than in the centre of an air space (see Figs. 5 & 6).

The computational process required about five hundred repetitions of the correction of temperatures and velocities at every control space. When solar radiation is strong, a strong air flow results, and calculations reach a stable condition with fewer repetitions.

The air velocity calculation showed a character of strong convergence, compared with the stability of heat balance calculations.

For a typical application, the height of an air space is expected to be the same height as an ordinary building floor height, i.e. 2.5 to 3 meters. The ratio of height-to-thickness of an air space then is about 100 for an air space thickness of 25 to 30 mm. Edge effect must be considered at the entrance region for a length of several times that of an air space thickness; however, the height of an air space is assumed to be long enough to neglect edge effect for the air flow in a space.

3. EXPERIMENTAL WORK WITH A FULL SCALE MODEL

To verify the computed heat and air flows, a full scale model test was carried out under external environmental conditions. This model was placed on the roof of the Centre for Building Studies, Concordia University, Montréal. The model was a box, with a height of 2.5 meter, depth of 3.0 meters and width of 1.2 meters, having a sloping roof. The box was a wood frame structure, with both sides of the framework covered by weatherproof

plywood sheets of 19 mm thickness. For this experiment, the spaces between the plywood plates, of depth 89 mm, on the south side wall was insulated with glass wool. The wall consisted of three experimental zones, each of width 406 mm and four control zones of width 406 mm at both sides and between the three experimental zones.

The siding used was aluminum plate, having a thickness of 0.3 mm, coated on both sides with dark brown paint. Each plate had a width of 406 mm and had three grooves of width 20 mm and depth 15 mm at an equal space along its length.

These plates were attached on the south wall with the grooves arranged vertically. The framework to attach the siding were square timbers of section 19 mm by 28 mm and directly attached at the top and bottom wall surface. The vertical distance between the top and bottom frame was 2.40 meters. Small openings were arranged on the frame of the two experimental zones. The openings for zone one consisted of twelve holes of diameter 15 mm and the openings for zone two were fifteen holes of diameter 6.35 mm. These opening areas correspond to 19% and 4% respectively, of the sectional areas of the air passages. The perimeter of zone three was carefully sealed with synthetic sealant.

On the vertical center line of each experimental zone, temperature sensors were arranged at the vertical height and 711 mm above and beneath the middle height. Temperature sensors were also arranged on the back surfaces of the siding and in air spaces 5 and 14 mm from the surface of the main wall.

For these temperature measurements, copper-constantan thermocouples of diameter 0.3 mm were used. Surface temperature measurements were monitored by wires for about 50 mm from the temperature-sensing junctions.

The incident radiative energy was not measured in this test; instead, the radiative incidence was calculated using the measured temperatures from the heat balance of the third experimental zone, the air space of which was sealed. The radiative incident heat was compared with the values calculated by the method used in ASHRAE Handbook of Fundamentals (see Table 1). In this calculation, the reflection term from the ground was halved in consideration of a small shaded wall which stood four meters from the experimental wall. The experimental and theoretical radiative incidents coincided well with each other at the thirteenth hour, as did their totals; however, the experimental radiative incident was generally smaller in the morning and larger in the afternoon. The roof, on which the experimental model was placed was finished with pebble surfaced asphalt roll roofing on a metal and an insulation plate. Its surface temperature rose in the afternoon, and the re-radiation from the roof surface seems to have had an influence on the radiative incident on the siding surface. For this reason, the experimentally attained radiation incident was used for the examination of the simulation of heat and air flow in the back space of the sidings of the experimental model. Both sides of the siding were coated with dark brown paint. The plywood surface of the main wall was exposed to outdoor air for five months before the experiment. The absorptance of the four surfaces was assumed to be 0.9. The other thermal constants of the materials used in the experimental model were taken from the ASHRAE Hand-

book of Fundamentals. The physical characters of the air were referred from handbooks of physics, and were evaluated at the mean temperature in the experimental work.

The measured and simulated temperature changes of the surface and air at the centre of the air space in experimental zone I is compared in (Fig. 3) by using the abscissa as the time axis. The simulated surface temperature change coincides well with the measured surface temperature change. However, the measured air temperature change at all the three measuring points fell in the range between the simulated temperature change at the middle and upper measuring points. The measured air temperature was three to six degrees Celsius higher than the simulated temperature of the corresponding measuring points.

The measured and simulated temperature changes of experimental zone II are compared in (Fig. 4). The measured surface temperatures showed one to three degrees Celsius higher values than the simulated values of corresponding times and positions. Measured air temperature at all three heights were about one degree Celsius lower than the simulated temperature for middle and top heights. The measured air temperature change at the lowest measuring point showed two to four degrees Celsius higher values than the simulated temperature change.

The higher air temperature in the experiment may mean :

a) The assumption of laminar flow in the air space is not suitable;

b) Turbulent conditions are caused by the air passage restriction on the frame at the bottom of the air space;

c) The air flow in the space was not as strong as predicted;

d) The heat exchange between the surface and the air in the space is increased by turbulent conditions.

The above points will be discussed in Section 5.

4. RESULTS OF COMPUTER SIMULATION

4.1 Ventilation Effect on Opaque Walls

Predictions for the efficacy of the air space ventilation is examined by entering various conditions of a typical wall structiure and orientation into the computer program. The location of a building for this simulation was chosen at a place of latitude 40° north; this enabled the computer simulation to be compared with solar heat gain calculation data presented in the ASHRAE Handbook of Fundamentals. Solar heat gain factors are taken from the July 21 data of Table 6, and Sol-air temperatures are taken from Table 26 of Chapter 22, of the Handbook'72; they were modified to meet the conditions of heat transfer at a siding surface. The temperature and radiative heat incident data, which were used for this simulation, are shown in Table 2.

The temperature distribution in an air space, siding, and external surfaces of a main wall is shown in (Fig. 5). The conditions for this case are : wall height - 2.4 meters, air space thickness - 30 mm, thermal conductance of the main wall - 0.358 watts/m^2.K, and radiative heat incidence - 322 watts/m^2. The aspect ratio of the air space in (Fig. 5) is distorted for illustrative convenience. The surface temperature of the siding is about three degrees Celsius higher than the external surface of the main

wall, although the peaks of the isotherm contours deviate to the main wall's side because the air velocity is higher at the siding's side.

The change in air velocity distribution with time is shown in (Fig. 6). The peak air velocity in the air space is displaced from the center of the space to the siding's side as the radiative heat incidence is increased. The air velocity distribution at 11:00 a.m. corresponds to the temperature distribution of (Fig. 5). The air temperatrue in the siding's surface is higher than that of the main wall's surface. This causes imbalance in buoyancy force through the space, and consequently the air velocity towards the siding is larger than that towards the main wall.

As radiative heat transfer takes place between the siding and main wall surfaces, the temperatures of the siding and of air space side surface of the main wall become higher than that in the air space. This causes reversal of heat flow direction at the air space side surface of the main wall. The heat which is transmitted by radiation to this surface is absorbed by the air stream in the space, and then released to the external environment.

The heat, incident on the siding surface as radiative energy, is traced in Table 3. The conditions of this calculation are the same as those used in (Fig. 5). During the period of 6 a.m. to 6 p.m., a total radiative heat of 1944 watt hours/m^2 was absorbed by the siding, of which 1726 watt hours/m^2 are dissipated to the outside from the outer surface of the siding by convection and radiation, and 169 watt hours/m^2 are transmitted into the room through the main wall. When this siding is not applied, 66.9 watt hours/m^2 are transmitted into the room, as is calculated from the Sol-air

temperature method. This indicates that the naturally ventilated air space saves 31% of the cooling load which would otherwise be transmitted through the wall of conductance 0.35 w/m^2. When the same siding is used, but the back space is sealed, the transmitted heat becomes 64.0 watt hours/m^2. Employing this value as the reference for the above comparison, the cooling load saving by siding ventilation is 28%.

Table 4 shows the average values of air velocity, friction loss, dynamic loss and Reynold's number for the above case. At times of high air velocity, dynamic loss at the holes on framework exceeds 50% of the total force, and Reynold's number exceeds 400. When the passage restriction is not as much, dynamic loss is considerably smaller than the friction loss. Air velocity is increased and Reynold's number exceeds 1000 in the times of high radiative incidence.

Tables 5, 6 and 7 show time-to-time heat transmission into the building through various space and opening configurations. Table 5 shows the case of no obstruction throughout the air passage. The depth of air space is changed from 20 mm to 50 mm.

Of the heat transmission values, the values with (a) indicate the case when the Reynold's number exceeded the critical value. When the depth of air space is 40 mm, the total heat transmission is reduced to 65% of the heat calculated with an external wall of the same type, in the absence of a siding. As the depth of the air space is reduced, the ventilation effect is reduced; the cooling load reduction is also decreased.

Table 6 shows the case when the total area of air passage is restricted to 50% of the sectional area of the enclosed space. A contraction coeffi-

cient of 0.6 was applied in considering the flow passage contraction at the openings, and the proportion of total heat transmission falls to 71% of the total heat transmission of the same wall but without siding.

Figure 7 shows the same case except that the air passage is further restricted to 25% of the sectional area.

As the depth of an air passage is increased, the effect of ventilation of the increases; however, this effect ceased to be of benefit when the depth reaches a certain value.

Table 8 shows the effect of main wall thermal resistance on the total heat transmission of ventilated air space walls. As the thermal resistance of the main wall increases, the effectiveness of the air space ventilation is reduced. However, 20% is still attainable for a main wall of thermal resistance 5.12 m^2k/w.

In Table 9, the effect of siding surfaces is examined. The value in the first column is calculated by using 0.9 for the emissivities of two surfaces of the siding and the outer surface of the main wall; this value applies for ordinary surfaces of building materials. In the second column, the emissivity of the back surface of a siding is changed to 0.4; this value corresponds to a metallic paint surface or a roughened aggravated metal surface. The third column is calculated for a siding with metallic surfaces on both sides. When the total heat transmission during 6 a.m. through 8 p.m. of each case is compared with the total heat transmission of a wall without this siding, and the emissivity of the external surface of it is 0.9, the effect of a siding and air space ventilation is found to be large.

Tables 10 and 11 show the transmitted heat through east and west oriented walls, respectively.

4.2 Ventilation Effect on Triple-Glazing

A large part of solar gain in normal buildings is caused by fenestration through windows. The thermal performance of a window is very much different from that of an opaque wall, and to utilize this simulation method on solar heat gain through a window, several assumptions were made, namely :

a) A triple-glazed window is the study subject, and the outermost glass is of heat absorbing type. The middle and inner glasses are clear plates and the space of 12.7 mm between them is completely sealed.

b) The transmitted radiation through the heat absorbing glass passes completely through the remaining part of the triple glazing. This part directly becomes cooling load.

c) The heat absorbed by the heat absorbing glass produces long wave radiation, and the clear plates are completely opaque for this spectral range of radiation.

Under these assumptions, the absorbed heat by the heat absorbing glass is treated, and heat transmission through the glazing is calculated by the simulation program. The short wave transmission is calculated separately. The short-wave transmission and the long-wave transmission compose the total heat gain through a window.

Further assumptions are : The heat absorption glass is at the one temperature. Here, the heat conductance of the glass is assumed to be small enough compared with that of the air films on both sides.

The inward long-wave re-radiation from the heat absorbing glass is absorbed completely by the middle glass. The temperature gradient in this glass is assumed to be negligible, because the conductance of the sealed air space is sufficiently larger than that of the middle glass.

The same radiative heat incidence as shown in Table 2 was applied. The incident angle was calculated from time to time, and the absorptance and transmittance of a heat-absorbing glass were read from (Fig. 5) of Chapter 22, ASHRAE Handbook of Fundamentals, 1972.

The trace of radiative heat incidence is shown in Table 12. The simulation subject is a south oriented window with an air space 30 mm between the heat absorbing glass and the middle glass. The total opening area of the air space is 50% of the sectional area of the air space. The total of direct heat transmission and indirect heat transmission, which is once absorbed by heat absorption glass, is 612 wH/m^2 for the period of 6 a.m. through 6 p.m. The heat transmission through double glazing, which has a sealed air space of thickness 12.5 mm, is calculated to be 801 wH/m^2 for the same period. The heat transmission through a triple-glazing, both air spaces sealed, results in 680 wH/m^2 for the same period (Table 13).

The heat transmission through a ventilated air space triple window corresponds to 76% of that of a double-glazed unit.

5. DISCUSSION AND CONCLUSION

The computer simulation assumes a laminar flow regime in the air passage, although result comparisons suggest that this may not be the case. The computer simulation showed also that when the thickness of an air space

exceeds 50 mm, the critical Reynold's number is exceeded in a strong radiation period; thus, turbulent flow must be considered. Practically, an entrance passage restriction may cause disturbance in the air flow. Consequently, the flow is believed to belong in the turbulent range for more occasions than is suggested by the computer simulation prediction.

The following may be deduced from the result of the simulation and experimental works.

When the air flow is in a turbulent regime, the ventilation effect of an air space is influenced both positively and negatively with respect to a comparison with the computer simulation using laminar flow theory. The heat exchange between a wall surface and the air in the air space becomes considerably greater than during laminar flow; this increases the air temperature and consequently, the force to move the air upward. However, the friction loss at a wall surface is also increased; thus, the estimation of the effect of air space ventilation by a laminar flow theory may not be very much different from actual conditions.

The high air temperature found in the experimental work shows that a potential force exists to motivate upward air flow. This ventilation works effectively in reducing cooling load, when a siding and an air passage are arranged to optimally utilize this natural force of buoyancy.

As the computer simulation based on the laminar flow theory indicated, the ventilation of the back space of siding by natural force has a potential for cooling load reduction on both opaque and transparent building enclosures, but the analysis remains to be developed fully to optimally employ this technique.

From the above results, the effect of air space ventilation seems potentially significant for cooling load reduction of buildings, the method being particularly attractive because it is passive.

6. REFERENCES

1. Vennard, J.K., Elementary Fluid Mechanics, John Wiley and Sons, Inc., New York, 1962.

2. Kaufmann, W., Fluid Mechanics, McGraw-Hill Book Co., Inc., New York, 1963.

3. Grober, H., Erk, S. and Grigwell, U., Fundamentals of Heat Transfer, McGraw-Hill Book Co., Inc., New York, 1961.

4. ASHRAE, Handbook of Fundamentals, American Society of Heating, Refrigerating and Air-Conditioning Engineers, 1972.

TABLE 1 - RADIATION INCIDENCE ON EXPERIMENTAL MODEL, AUGUST 17, 1979

TIME	a) CALCULATED FROM HEAT BALANCE OF SEALED SECTION w/m^2	b) CALCULATED BY ASHRAE METHOD w/m^2	a) - b) w/m^2
10	283	520	-237
11	404	601	-187
12	512	629	-117
13	612	601	+ 20
14	680	529	+160
15	545	392	+153
16	377	240	+137
17	288	74	+214
TOTAL*	3,702 WH/m^2	3,577 WH/m^2	+133 WH/m^2 (+3.6%)

* TOTAL OF 7 HOURS

TABLE 2 - TEMPERATURE AND RADIATION INCIDENCE DATA FOR 40° NORTH LATITUDE ON JULY 21

TIME	AIR TEMP. °C	RADIATION w/m^2			SOL AIR TEMPERATURE°C		
		EAST WALL	SOUTH WALL	WEST WALL	EAST	SOUTH	WEST
6	23.3	432	32	32	42.8	24.4	24.4
7	23.9	643	63	60	52.5	26.7	26.7
8	25.0	688	91	82	55.8	30.0	28.6
9	26.7	611	164	98	55.0	36.9	31.1
10	28.3	460	252	110	50.8	42.8	33.3
11	30.6	255	322	117	45.0	48.1	35.8
12	32.3	129	344	129	32.1	50.6	38.1
13	33.9	117	322	255	39.2	51.4	48.3
14	39.4	110	252	460	39.4	48.9	56.9
15	35.0	98	164	611	39.4	45.3	63.3
16	34.4	82	90	681	38.1	39.4	65.3
17	33.9	60	63	643	36.7	36.7	62.5
18	32.8	32	32	432	33.9	33.9	52.5

CONVERTED FROM TABLES 4 AND 26 OF CH. 22, ASHRAE HANDBOOK OF FUNDAMENTALS, 1972.

TABLE 3 - TRACE OF RADIATIVE HEAT INCIDENCE

SOUTH WALL, AIR SPACE THICKNESS 30 mm
PROPORTION OF TOTAL OPENING AREA 50%
OTHER CONDITIONS - SEE TABLE 5

TIME	AIR TEMPERATURE	ABSORBED RADIATION w/m^2	DISSIPATION FROM OUTER SURFACE w/m^2	DISSIPATION BY AIR CHANGE w/m^2	TRANSMITTED INTO ROOM w/m^2
6	23.3	28.8	27.4	1.2	.1
7	23.9	56.7	52.7	3.4	.6
8	25.0	81.7	75.1	5.6	1.3
9	26.7	147.6	132.8	12.2	2.5
10	28.3	226.8	201.5	21.3	3.7
11	30.6	289.8	255.5	28.8	5.1
12	32.2	309.6	272.3	31.0	5.8
13	33.9	289.8	255.1	28.1	6.1
14	34.4	226.8	200.6	20.2	5.7
15	35.0	147.6	131.3	11.1	5.2
16	34.4	81.0	72.2	4.4	4.3
17	33.9	56.7	59.4	2.4	3.9
18	32.8	28.8	25.0	0.6	3.2
TOTAL* wH/m^2		1944.0	1725.7	169.4	45.9

* TOTAL OF 12 HOURS

TABLE 4 - CHARACTERISTICS OF AIR FLOW

40°N, JULY 21, CONDUCTANCE WALL 0.358 w/m^2K
SOUTH WALL, DEPTH OF AIR SPACE 30 mm
EMISSIVITIES OF SURFACES 0.9
PROPORTION OF TOTAL OPENING ARE 50%
OTHER CONDITIONS - SEE TABLE 5

TIME	AVERAGE VELOCITY m/s	FRICTION LOSS N/m^2	DYNAMIC LOSS N/m^2	REYNOLD'S NO.
6	0.06	0.066	.029	129
7	0.100	0.102	.064	189
8	0.121	0.128	.094	228
9	0.164	0.186	.169	304
10	0.201	0.241	.255	369
11	0.224	0.287	.318	408
12	0.231	0.298	.336	416
13	0.222	0.282	.312	400
14	0.196	0.237	.244	355
15	0.157	0.175	.156	283
16	0.111	0.114	.078	202
17	0.088	0.087	.049	161
18	0.052	0.049	.017	95

TABLE 5 - PERFORMANCE OF VENTILATED AIR SPACE WALL

TIME	AIR SPACE THICKNESS mm					
	10	20	30	40	50	
	Heat Transmission into room w/m^2					
6	.2	.2	.1	.1	.1	
7	.8	.7	.6	.6	.5	
8	1.5	1.3	1.2	1.1	1.1	
9	2.9	2.5	2.3	2.3	2.3	
10	4.5	3.8	3.5	3.5	3.5	(a)
11	6.0	5.1	4.8	4.7	4.7	(a)
12	6.8	5.8	5.5	5.4	5.4	(a)
13	7.1	6.2	5.9	5.8	5.8	(a)
14	6.5	5.8	5.5	5.5	5.5	(a)
15	5.6	5.3	5.3	5.0	5.0	
16	4.5	4.4	4.2	4.2	4.2	
17	4.0	3.9	3.8	3.8	3.8	
18	2.3	3.2	3.2	3.2	3.2	
TOTAL*	52.0	46.5	44.0	43.6	43.5 wH/m^2	
proportion to a)**	78%	70%	66%	65%	65%	

CONDITIONS

LOCATION	: 40° NORTH LATITUDE
DATE	: JULY 21
ORIENTATION OF WALL	: SOUTH
HEIGHT OF AIR SPACE	: 2.4 m
THERMAL CONDUCTANCE OF MAIN WALL	: 0.358 W/m^2K
PROPORTION OF TOTAL OPENING AREA TO VERTICAL SECTIONAL AREA OF AIR SPACE	: 100%
INDOOR AIR TEMPERATURE	: 24°C
EMISSIVITY OF SURFACE	: OUTER SURFACE OF SIDING 0.9
	: INNER SURFACE OF SIDING 0.9
	: OUTER SURFACE OF MAIN WALL 0.9

* TOTAL : TOTAL FOR 12 HOURS OF 6 HOUR THROUGH 18 HOUR, IN wH/m^2

** CASE a) : CALCULATED HEAT TRANSMISSION INTO ROOM FOR THE SAME CASE AS THIS, BUT WITHOUT SIDING, USING SOL-AIR TEMPERATURE

TABLE 6 - PERFORMANCE OF VENTILATED AIR SPACE WALL

PROPORTION OF OPENING - 50%
OTHER CONDITIONS, SEE TABLE 5

TIME	DEPTH OF AIR SPACE IN mm							
	10	20	30	40	50	65	80	100
	Heat Transmission into room w/m^2							
6	.2	.2	.1	.1	.1	.1	.1	.1
7	.8	.7	.6	.6	.6	.6	.6	.6
8	1.5	1.4	1.2	1.2	1.2	1.2	1.2	1.2
9	2.9	2.6	2.4	2.4	2.4	2.4	2.4	2.4
10	4.5	4.0	3.7	3.7	3.6	3.6	3.6	3.7 (a)
11	6.0	5.3	4.0	4.0	5.0	5.0	5.0	5.0 (a)
12	6.8	6.1	4.7	4.7	5.7	5.7	5.7	5.7 (a)
13	7.1	6.4	6.1	6.1	6.0	6.0	6.1	6.1 (a)
14	6.5	6.0	5.7	5.7	5.6	5.6	5.6	5.6 (a)
15	5.6	5.3	5.2	5.1	5.1	5.1	5.1	5.1
16	4.5	4.4	4.3	4.3	4.2	4.2	4.2	4.2
17	4.0	3.9	3.8	3.8	3.8	3.8	3.8	3.8
18	3.3	3.2	3.2	3.2	3.2	3.2	3.2	3.2
TOTAL*	53.7	47.8	45.8	46.9	46.5	46.5	46.6	46.7
Proportion to a)**	.82	.75	.72	.71	.71	.71	.71	.71

a) SHOWS THE CASE WHEN REYNOLD'S NUMBER EXCEEDS 1000

* TOTAL HEAT TRANSMISSION OF PERIOD OF 6 HOUR THROUGH 18 HOUR, IN wH/m^2

TABLE 7 - PERFORMANCE OF VENTILATED AIR SPACE WALL

PROPORTION OF OPENING - 25%
OTHER CONDITIONS, SEE TABLE 5

TIME	DEPTH OF AIR SPACE IN mm							
	10	20	30	40	50	65	80	100
	Heat Transmission into room w/m^2							
6	.2	.2	.1	.1	.1	.1	.1	.1
7	.8	.7	.7	.6	.6	.6	.6	.6
8	1.5	1.4	1.3	1.3	1.3	1.2	1.2	1.2
9	2.9	2.7	2.6	2.5	2.5	2.5	3.5	2.5
10	4.5	4.2	4.0	3.9	3.8	3.8	3.8	3.8
11	6.1	5.6	5.3	5.2	5.2	5.2	5.2 (a)	5.2 (a)
12	6.9	6.3	6.1	6.0	5.9	5.9	5.9 (a)	5.9 (a)
13	7.2	6.7	6.4	6.3	6.3	6.3	6.2 (a)	6.2 (a)
14	6.5	6.1	5.9	5.9	5.8	5.8	5.8	5.8 (a)
15	5.6	5.4	5.3	5.2	5.2	5.2	5.2	5.2
16	4.5	4.4	4.2	4.3	4.3	4.3	4.3	4.3
17	4.0	3.9	3.9	3.9	3.9	3.8	3.8	3.8
18	3.3	3.2	3.2	3.2	3.2	3.2	3.2	3.2
TOTAL*	54.0	50.8	49.1	48.4	48.1	47.8	47.8	47.8 wH/m^2
Proportion to a)**	.82	.77	.75	.74	.73	.73	.73	.73

TABLE 8 - EFFECT OF THERMAL RESISTANCES OF MAIN WALLS ON HEAT TRANSMISSION INTO A ROOM

AIR SPACE THICKNESS - 50 mm
PROPORTION OF TOTAL OPERNING AREA - 50%
OTHER CONDITIONS - SEE TABLE 5

TIME	THERMAL RESISTANCE OF MAIN WALL IN m^2K/w		
	1.56	2.79	5.12
6	.2	.1	.1
7	1.0	.6	.4
8	2.0	1.2	.8
9	4.0	2.4	1.5
10	6.1	3.6	2.3
11	8.3	5.0	3.2
12	9.5	5.7	3.6
13	10.1	6.0	3.8
14	9.4	5.6	2.6
15	8.5	5.1	3.2
16	7.0	4.2	2.7
17	6.4	3.8	2.4
18	5.3	3.2	2.0
TOTAL* wH/m^2	75.1	46.5	28.6
Proportion to a**	.68	.71	.80

TABLE 9 - EFFECT OF EMISSIVITY OF SIDING SURFACES ON THE HEAT TRANSMISSION INTO A ROOM

AIR SPACE THICKNESS - 50 mm
PROPORTION OF TOTAL OPENING AREA - 255
OTHER CONDITIONS - SEE TABLE 5

TIME	POSITION	EMISSIVITY		
	Siding outer surface Siding inner surface	0.9 0.9	0.9 0.4	0.4 0.4
	Heat transmission into a room in w/m^2			
6		.1	.1	-0.1
7		.6	.5	.2
8		1.3	1.1	.7
9		2.5	2.2	1.5
10		3.8	3.4	2.0
11		5.2	4.6	3.3
12		5.9	5.3	3.9
13		6.3	5.7	4.3
14		5.8	5.3	4.2
15		5.2	4.8	4.1
16		4.3	4.0	3.6
17		3.9	3.7	3.3
18		3.2	3.0	2.8
TOTAL*		48.1	42.2	32.8 wH/m^2
Proportion to case a**		.72	.63	.49

TABLE 10 - HEAT FLOW FOR EAST WALL

PROPORTION OF TOTAL OPENING AREA - 50%
OTHER CONDITIONS - SEE TABLE 5

TIME	THICKNESS OF AIR SPACE in mm		
	30	40	50
	Heat Transmission into room in w/m ^{2}		
6	3.5	3.5	3.4
7	5.4	5.3	5.3
8	6.0	5.9	5.9
9	6.1	6.0	5.9
10	5.4	5.3	5.4
11	4.5	4.4	4.4
12	3.9	3.9	3.9
13	4.4	4.3	4.3
14	4.5	4.4	4.4
15	4.6	4.5	4.5
16	4.2	4.2	4.2
17	3.8	3.8	3.8
18	3.2	3.2	3.2
TOTAL* wH/m ^{2}	56.1	55.4	55.2
Proportion to case a**	.69	.68	.68

TABLE 11 - HEAT FLOW FOR WEST WALL

PROPORTION OF TOTAL OPENING AREA - 50%
OTHER CONDITIONS - SEE TABLE 5

TIME	THICKNESS OF AIR SPACE in mm		
	30	40	50
	Heat Transmission into room in w/m^2		
6	0.1	0.1	0.1
7	0.6	0.6	0.6
8	1.2	1.1	1.1
9	1.9	1.8	1.8
10	2.5	2.5	2.4
11	3.3	3.3	3.2
12	3.9	3.9	3.9
13	5.6	5.5	5.5
14	7.4	7.3	7.3
15	8.8	8.7	8.7
16	9.1	9.0	9.0
17	8.7	8.6	8.6
18	6.7	6.6	6.6
TOTAL* wH/m^2	56.4	55.7	55.5
Proportion to case a**	.69	.68	.68

TABLE 12 - HEAT BALANCE OF VENTILATED TRIPPLE WINDOW

SOUTH WINDOW
AIR SPACE THICKNESS - 30 mm
PROPORTION OF TOTAL OPENING AREA - 50%
OTHER CONDITIONS - SEE TABLE 5

TIME	TRANSMITTED TO ROOM DIRECTLY w/m^2	ABSORBED BY FIRST GLASS w/m^2	DISSIPATED FROM OUTER SURFACE w/m^2	DISSIPATED BY AIR CHANGE w/m^2	TRANSMITTED TO ROOM INDIRECTLY w/m^2	TOTAL DIRECT AND INDIRECT w/m^2
6	3.2	3.2	4.1	0.1	-1.0	2.2
7	4.0	4.0	3.8	0.0	0.2	4.1
8	4.6	4.6	2.4	0.0	2.2	6.8
9	16.4	65.6	53.7	2.2	9.6	26.0
10	50.4	121.0	98.9	5.8	16.3	66.7
11	80.5	161.0	129.6	8.2	23.1	103.6
12	90.9	178.9	142.5	9.0	27.3	118.2
13	80.5	161.0	125.0	6.5	29.4	109.9
14	50.4	121.0	90.0	3.2	27.8	78.2
15	16.4	65.6	40.4	0.2	25.0	41.4
16	4.6	4.6	-14.5	0.0	19.1	23.7
17	4.0	4.0	-14.1	0.0	18.1	22.1
18	3.2	3.2	-12.9	0.0	16.1	19.3
TOTAL wH/m^2	405.9	894.5	653.3	35.2	205.6	611.5

Proportion to case a) - 76%

TABLE 13 - PERFORMANCE OF VENTILATED TRIPLE GLAZING

SOUTH WINDOW
PROPORTION OF TOTAL OPENING AREA - 50%
OTHER CONDITIONS - SEE TABLE 5

TIME	AIR SPACE THICKNESS		
	30 mm	40 mm	50 mm
	w/m^2	w/m^2	w/m^2
6	-1.0	-1.0	-1.0
7	.1	.1	.1
8	2.2	2.1	2.1
9	9.6	9.5	9.4
10	16.3	16.0	15.8
11	23.1	22.8	22.6
12	27.3	26.9	26.8
13	29.4	29.0	28.8
14	27.8	27.4	27.2
15	25.0	24.8	24.6
16	19.1	18.9	18.8
17	18.1	18.0	17.9
18	16.1	16.0	15.9
TOTAL :			
INDIRECT	205.6	203.0	201.7 WH/m^2
DIRECT	405.9	405.9	405.9 WH/m^2
TOTAL*	611.5	608.9	607.6 WH/m^2
Proportions to double ventilated glazing	.76	.76	.76

TABLE 14 - PERFORMANCE OF VENTILATED TRIPPLE GLAZING
HEAT TRANSMISSION INTO ROOM

SOUTH WINDOW
PROPORTION OF TOTAL OPENING AREA - 25%
OTHER CONDITIONS - SEE TABLE 5

TIME	AIR SPACE THICKNESS		
	30 mm	40 mm	50 mm
	w/m^2	w/m^2	w/m^2
6	-1.0	-1.0	-1.0
7	.1	.1	.1
8	2.2	2.1	2.1
9	9.8	9.6	9.5
10	16.8	16.3	16.2
11	23.6	23.2	23.0
12	27.8	27.4	27.1
13	29.8	29.3	29.1
14	27.9	27.6	27.4
15	25.0	24.8	24.6
16	19.1	18.9	18.8
17	18.1	18.0	17.9
18	16.1	16.0	15.9
TOTAL :			
INDIRECT	207.6	204.8	203.3 wH/m^2
DIRECT	405.9	405.9	405.9 wH/m^2
TOTAL*	613.5	610.7	609.2 wH/m^2
Proportions to double unventilated glazing	.77	.76	.76

LIST OF TABLES

LIST OF FIGURES

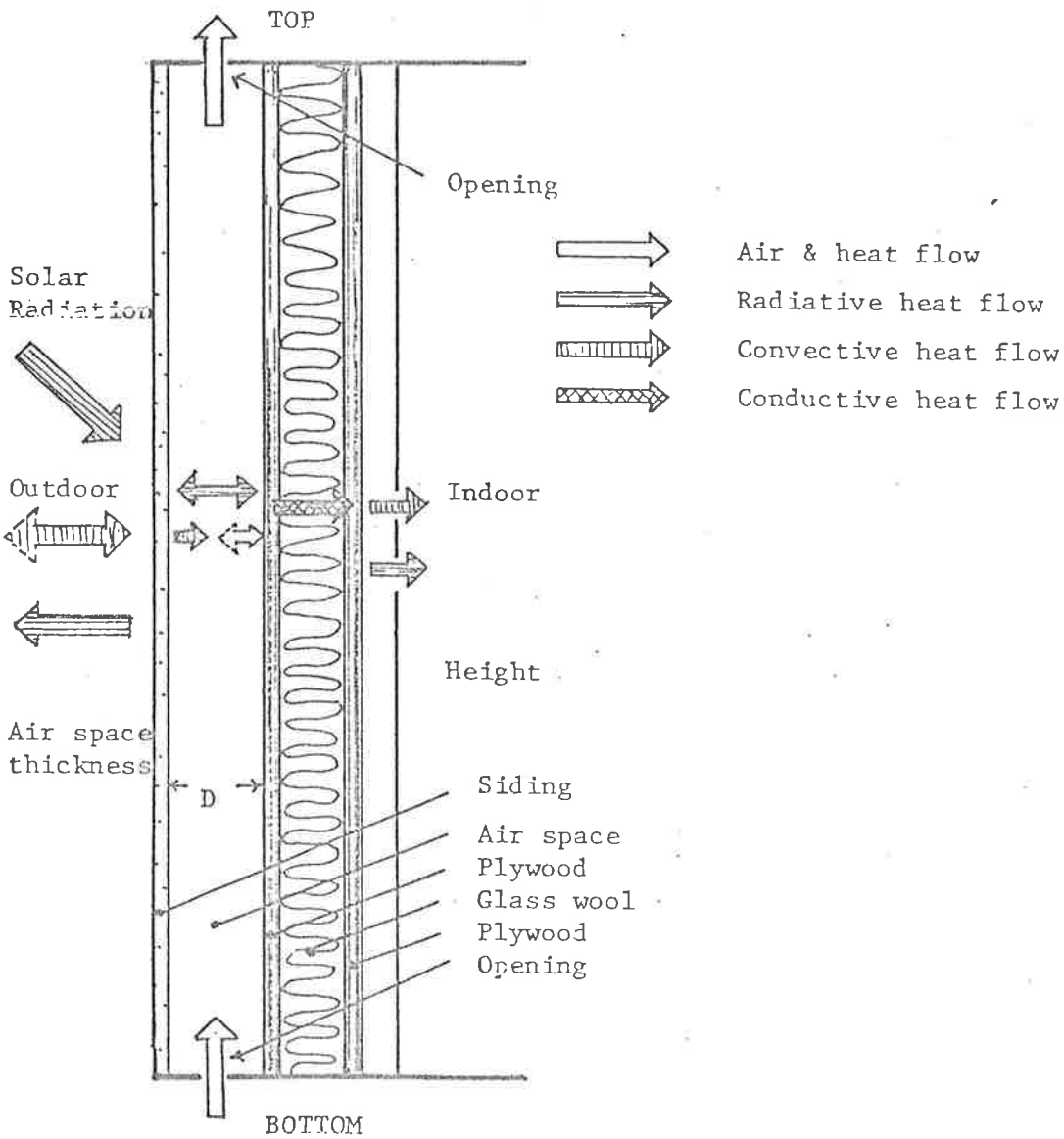

FIG. 1 - MODEL OF GROSS HEAT AND AIR FLOWS AT A WALL (VERTICAL SECTION)

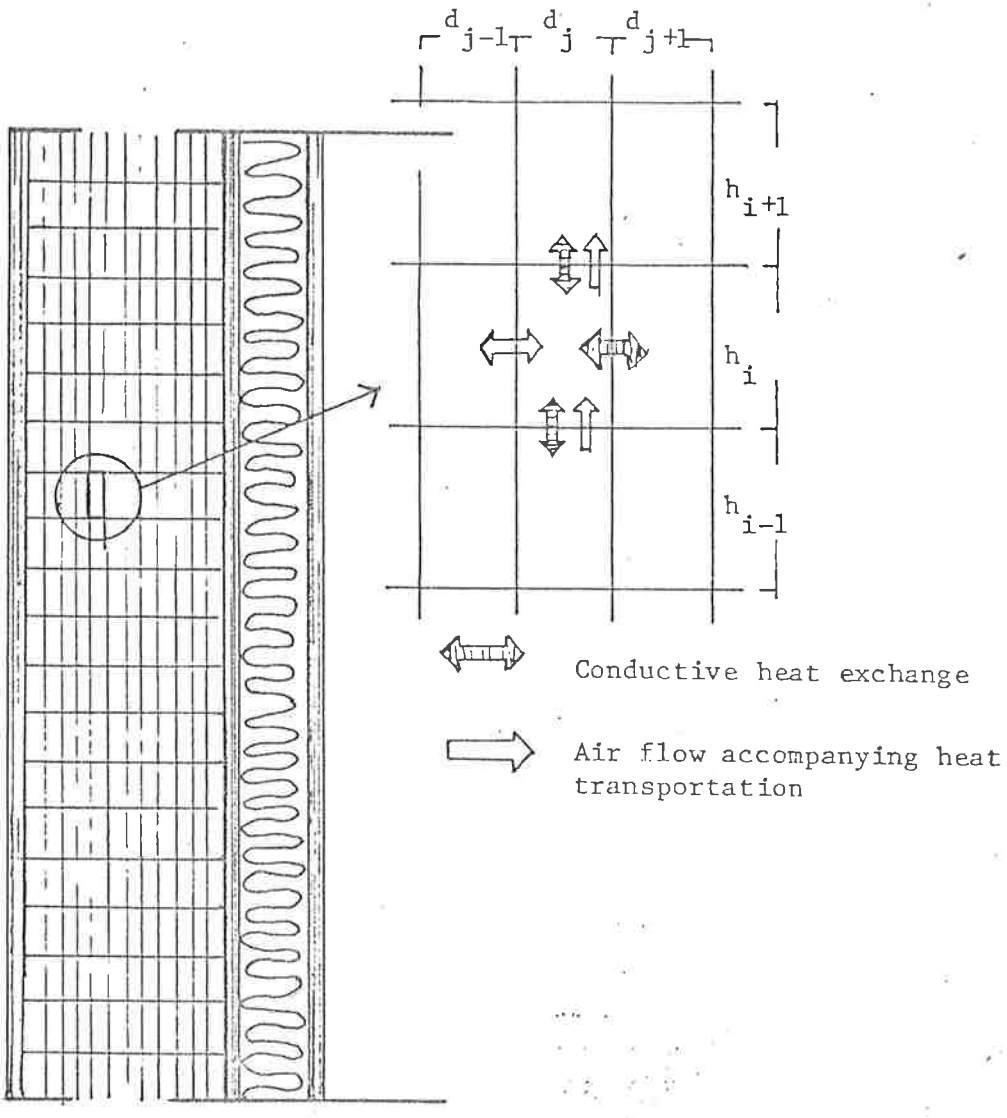

FIG. 2 – DIVISION OF AIR SPACES AND THEIR HEAT EXCHANGE

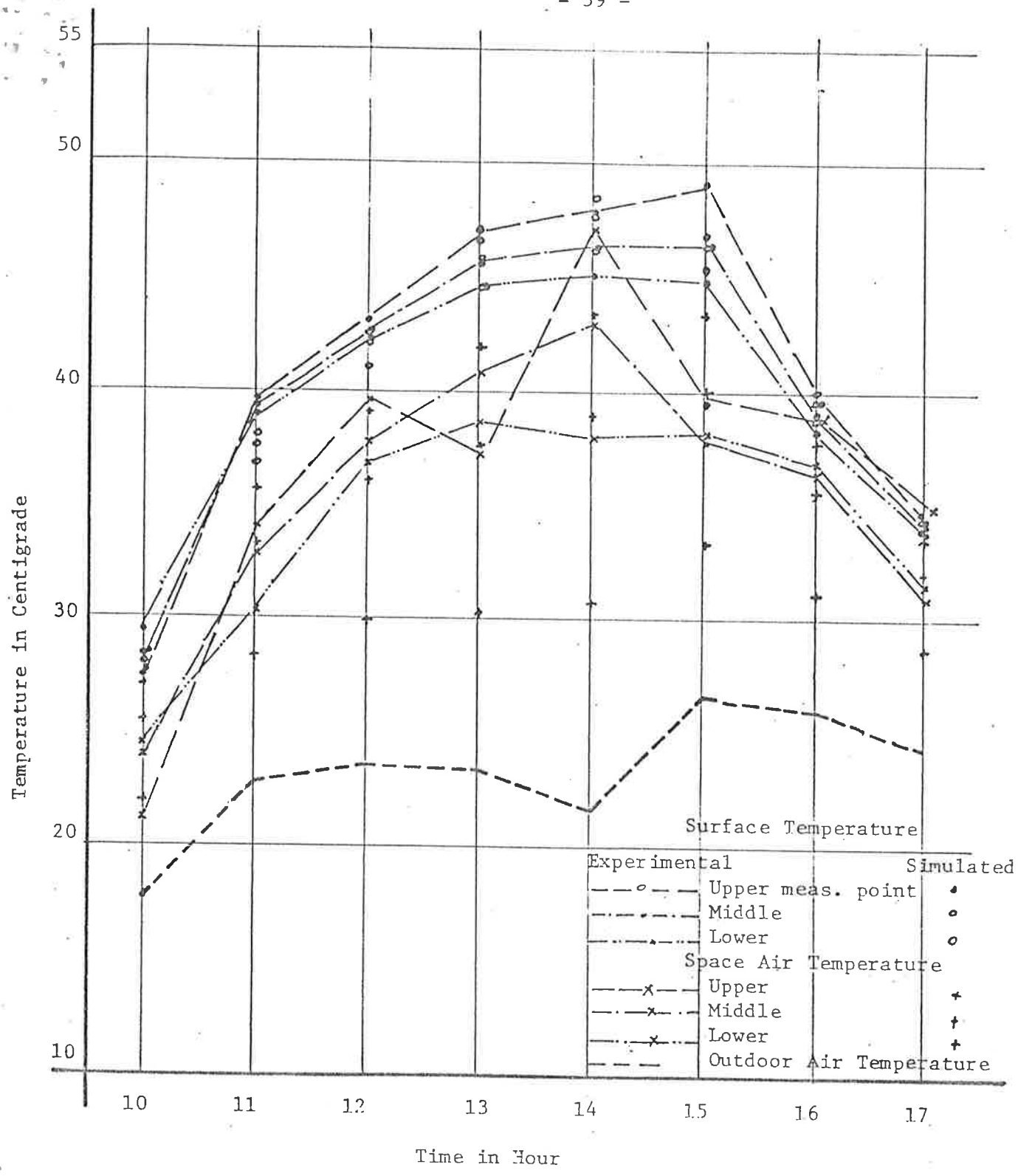

FIG. 3 - SURFACE AND AIR TEMPERATURE CHANGE OF EXPERIMENTAL ZONE I
PROPORTION OF TOTAL OPENING AREA TO SECTIONAL AREA
OF AIR SPACE - 19%

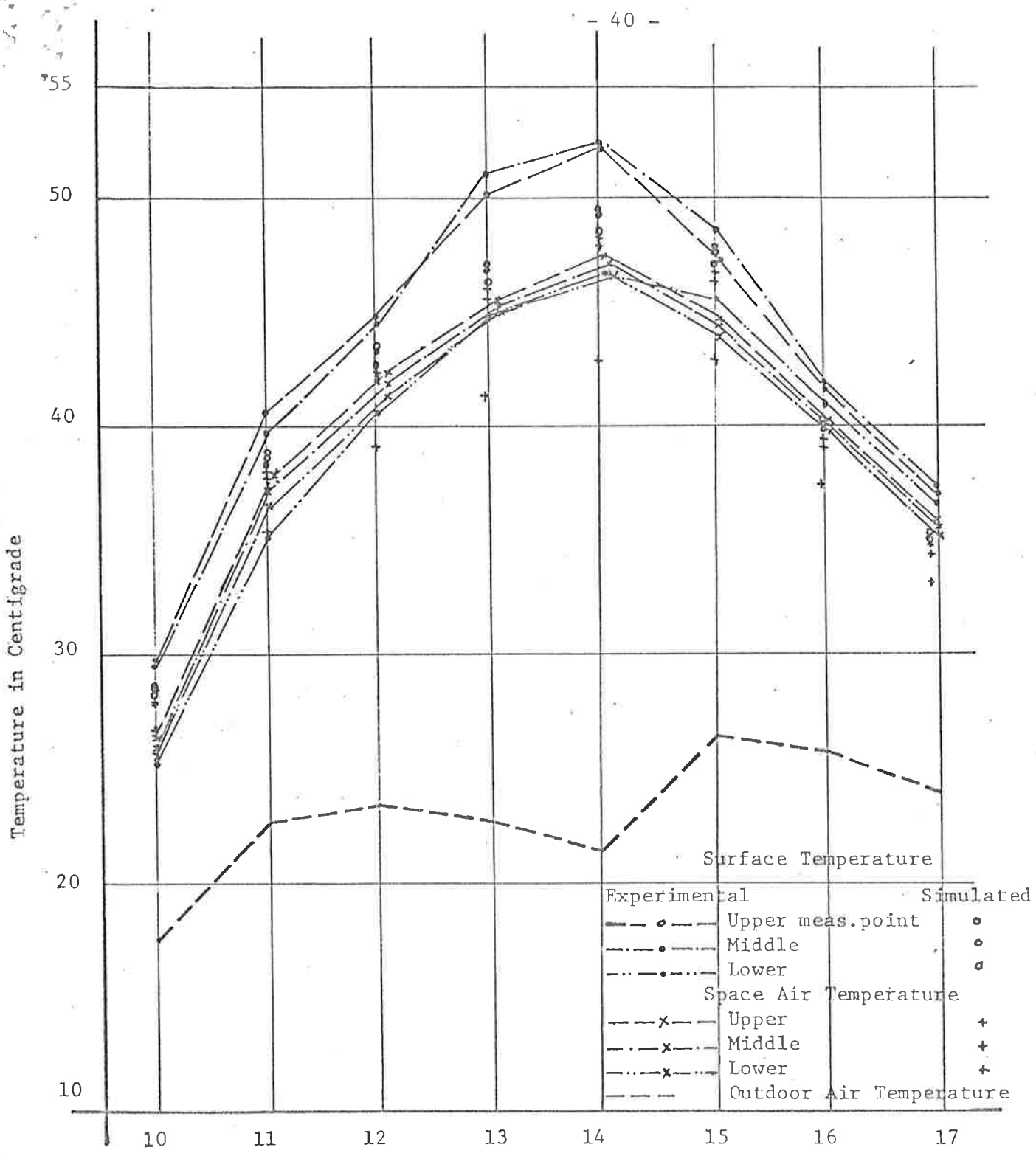

FIG. 4 - SURFACE AND AIR TEMPERATURE CHANGES OF EXPERIMENTAL ZONES II PROPORTION OF TOTAL OPENING AREA TO SECTIONAL AREA OF AIR SPACE - 4%

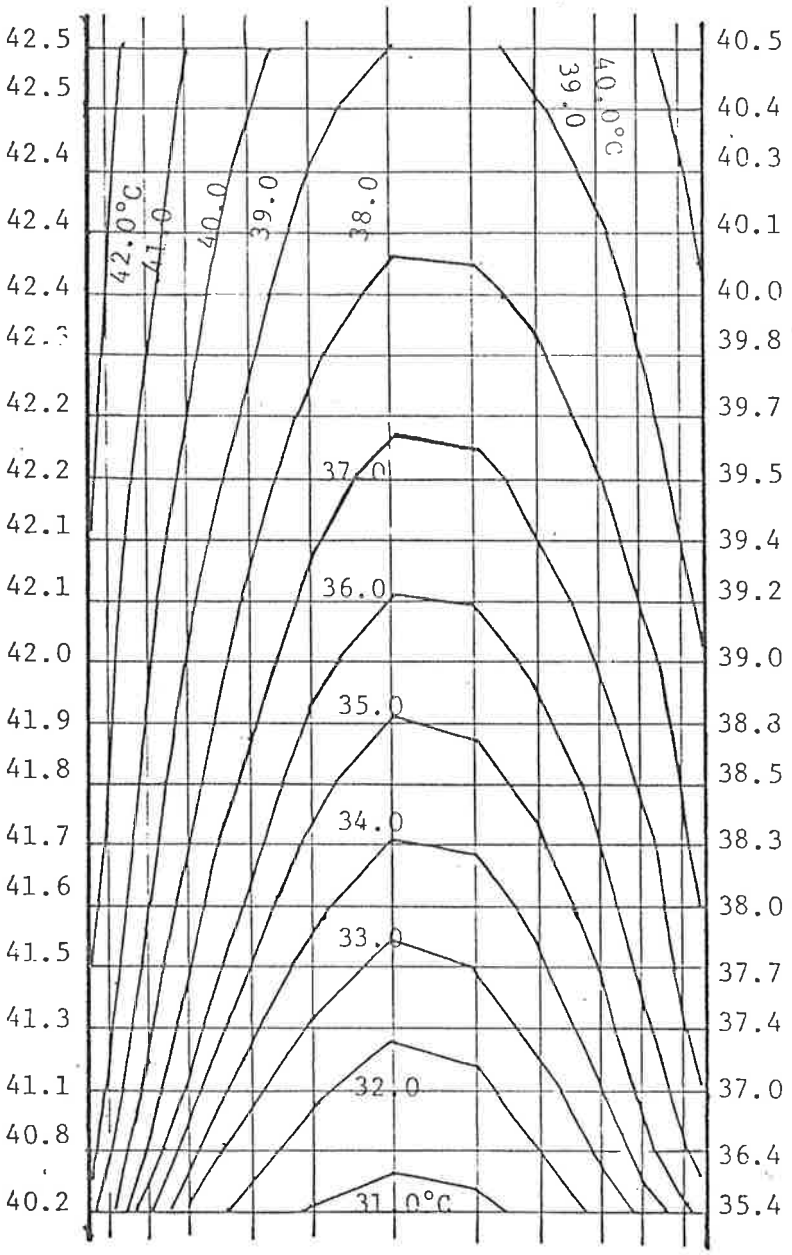

FIG. 5 - TEMPERATURE DISTRIBUTION IN AIR SPACE AND SURFACES (INFLOW AIR TEMPERATURE 30.6°C)

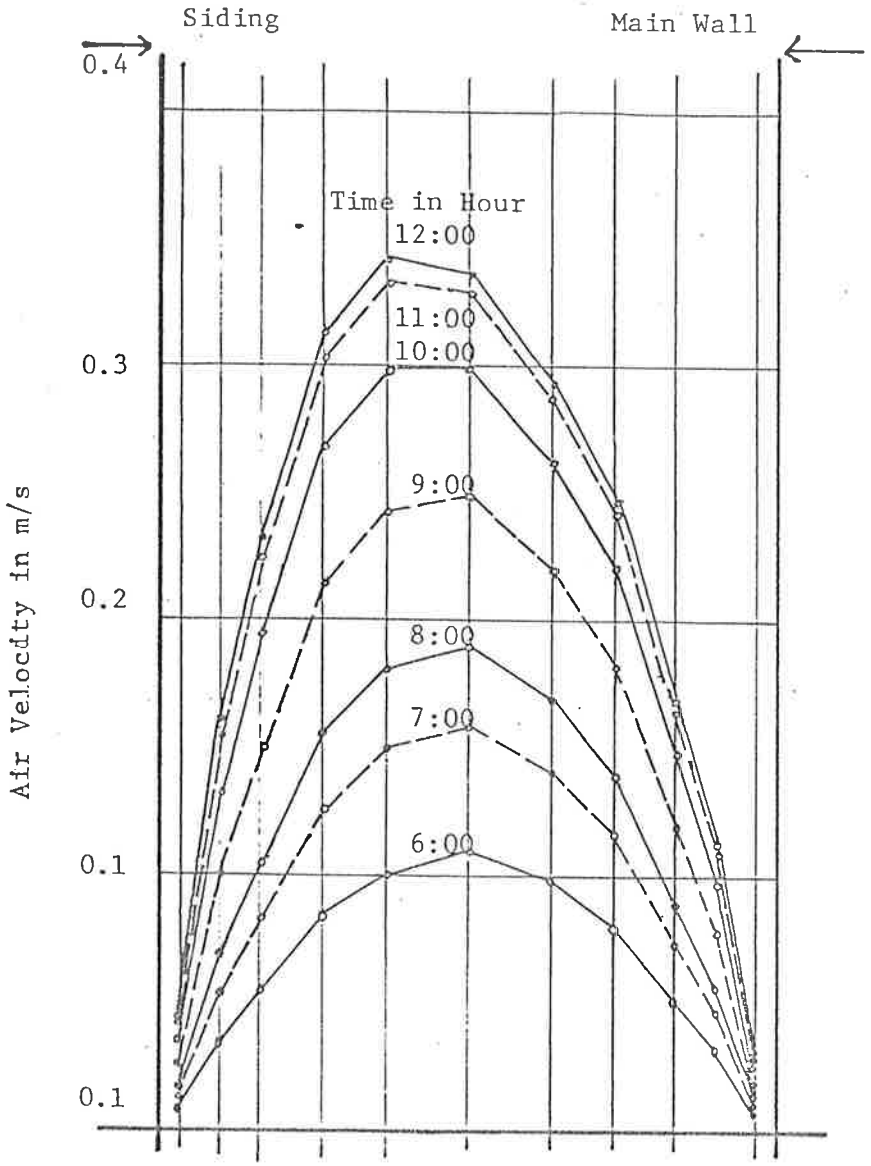

FIG. 6 - AIR VELOCITY DISTRIBUTION IN AIRSPACE